Aging Cell (2011) **10,** pp595–603 Doi: 10.1111/j.1474-9726.2011.00685.x

Membrane cholesterol content plays a key role in the neurotoxicity of β-amyloid: implications for Alzheimer's disease

Andrey Y. Abramov,[1] Maksim Ionov,[2] Evgeny Pavlov[3] and Michael R. Duchen[4]

[1]Department of Molecular Neuroscience, UCL Institute of Neurology, Queen Square, London WC1N 3BG, UK
[2]Department of General Biophysics, University of Lodz, Banacha st. 12/16, Lodz 90-237, Poland
[3]Department of Physiology and Biophysics, Dalhousie University, Halifax, NS, Canada
[4]Department of Cell and Developmental Biology and Consortium for Mitochondrial research, University College London, London WC1E 6BT, UK

Summary

Beta amyloid (βA) plays a central role in the pathogenesis of the most common and devastating neurodegenerative disorder, Alzheimer's disease (AD). The mechanisms of βA neurotoxicity remain controversial, but include dysregulation of calcium homeostasis and oxidative stress. A large body of data suggest that cholesterol plays a significant role in AD. In mixed cultures containing hippocampal neurons and astrocytes, we have shown that neurotoxic βA peptides (1–42 and 25–35) cause sporadic cytosolic calcium ($[Ca^{2+}]_c$) signals in astrocytes but not in neurons, initiating a cascade that ends in neuronal death. We now show, using the cholesterol-sensitive fluorescent probe, Filipin, that membrane cholesterol is significantly higher in astrocytes than in neurons and mediates the selective response of astrocytes to βA. Thus, lowering [cholesterol] using mevastatin, methyl-β-cyclodextrin or filipin prevented the βA-induced $[Ca^{2+}]_c$ signals, while increased membrane [cholesterol] increased βA-induced $[Ca^{2+}]_c$ signals in both neurons and astrocytes. Addition of βA to lipid bilayers caused the appearance of a conductance that was significantly higher in membranes containing cholesterol. Increasing membrane [cholesterol] significantly increased βA-induced neuronal and astrocytic death. We conclude that a high membrane [cholesterol] promotes βA incorporation into membranes and increased $[Ca^{2+}]_c$ leading to cell death.

Correspondence
Dr. Andrey Y. Abramov, Department of Molecular Neuroscience, UCL Institute of Neurology, Queen Square, London WC1N 3BG, UK. Tel.: +44 2078373611; fax: +44 207 278 5616; e-mail: a.abramov@ucl.ac.uk

Accepted for publication 9 *February 2011*

Key words: astrocyte; calcium; cholesterol; neurodegeneration; neuron; β-amyloid.

Introduction

Alzheimer's disease (AD) is the most common form of dementia currently affecting 12 million people worldwide, a figure which is estimated to nearly triple by 2050 (Citron, 2004). The characteristic histological features of the post-mortem brain of a patient with AD are neuritic (or senile) plaques and neurofibrillary tangles – the two pathological markers required to make a definitive clinical diagnosis of AD. Senile plaques are formed extracellularly and consist of insoluble aggregates of different isoforms (39–42 amino acids) of amyloid β (βA) peptide (Masters *et al.*, 1985; Haass & Selkoe, 2007). A substantial body of evidence suggests that βA peptide accumulation plays a major role in the pathophysiology of neurodegeneration in AD, hence the 'amyloid cascade hypothesis' of AD pathogenesis. Certainly, βA aggregates are major histological feature in the brains of patients with AD, and βA peptides are toxic to both cortical and hippocampal neurons *in vitro* and *in vivo* (Hardy & Selkoe, 2002). However, the fundamental mechanisms of βA neurotoxicity are not well understood. Several recapitulated themes to emerge in the literature involve descriptions of altered cellular calcium signalling (or 'dysregulation' of calcium homeostasis), altered glutamate transport, oxidative stress, altered cholesterol metabolism and alterations in the activity of a number of enzyme systems. The chain of causality and the specific relationship between these variables have remained elusive.

In the last few years, we have attempted to explore the mechanisms of βA neurotoxicity in a primary cell culture model in which neurons grow together with astrocytes. We have found that in these co-cultures, βA induces, after a delay of a few minutes, the appearance of sporadic and rather slow $[Ca^{2+}]_c$ transients in astrocytes but not in neurons (Abramov *et al.*, 2003, 2004b). Indeed, in the short term (over 1–2 h), we have seen no change in any aspect of neuronal physiology. The astrocytic $[Ca^{2+}]_c$ signals showed an absolute requirement for external calcium and involved a calcium influx pathway. Perhaps, most remarkably, although early signals were seen in astrocytes, at 24 h, we saw substantial neuronal and not astrocytic cell death. We also showed that suppression of βA-induced $[Ca^{2+}]_c$ signals in astrocytes could protect the neurons, suggesting a major role for the calcium signals as a trigger to neuronal death. We have therefore addressed the issue of how $[Ca^{2+}]_c$ signals in astrocytes might lead to neuronal death and found βA-induced oxidative stress and glutathione (GSH) depletion in astrocytes, which was depen-

Aging Cell

dent on Ca^{2+}-dependent activation of the Nicotinamide adenine dinucleotide phosphate (NADPH) oxidase (Nox) in astrocytes (Abramov *et al.*, 2004a; Abramov & Duchen, 2005). Neurons also became GSH depleted. These data suggested that neuronal death results from a failure of astrocytic trophic support [astrocytes provide GSH precursors to neurons – (Dringen & Hirrlinger, 2005)]. Neurons were protected by inhibition of the NADPH oxidase, by antioxidants and by provision of glutathione precursors, placing oxidative stress generated by the NADPH oxidase as a key mediator of βA-induced neurodegeneration.

Thus, βA-induced neurodegeneration seems to involve a cascade initiated by activation of $[Ca^{2+}]_c$ signals in astrocytes, Nox activation generating oxidative stress and mitochondrial dysfunction and disruption of antioxidant (GSH) defences in astrocytes and neurons, leading to neuronal death. However, many of the steps in the development of βA-induced neurodegeneration remain unclear. One of the central remaining questions in this scheme is why βA triggers $[Ca^{2+}]_c$ signals in astrocytes but not in neurons. βA can form Ca^{2+} permeant channels in lipid bilayers (Arispe *et al.*, 1993; Kagan *et al.*, 2004), but this pore-forming activity appears to be critically dependent on the cholesterol content of the membranes. Thus, it has been reported that the pore-forming activity of βA in lipid bilayers is inversely related to the cholesterol content of the lipid mixture (Kawahara *et al.*, 2000; Arispe & Doh, 2002). Depletion of cholesterol content in cells or inhibition of cholesterol synthesis in PC12 cells has been reported to increase βA toxicity (Arispe & Doh, 2002). It is therefore possible that the different effects of βA on different cell types are related to variations in the membrane lipid composition of different cells. Remarkably, the only factor known to cause a genetic predisposition to AD is the isoform of ApoE, a protein involved in cholesterol transport (Bignall, 1993).

We have therefore now used fluorescence imaging to investigate the interaction between the level of cholesterol in the membrane of neurons and astrocytes and the ability of βA to induce calcium signals and cell death in these cells and report a key role for membrane cholesterol content as a determinant of βA toxicity.

Results

Membrane cholesterol is higher in astrocytes than in neurons

The level of cholesterol in the membranes of primary cells in culture was measured using the cholesterol-specific fluorescent dye filipin (Norman *et al.*, 1972; Drabikowski *et al.*, 1973). Correlation of the filipin fluorescence and the transmitted light image was used to help identify neurons and astrocytes as the appearance of the two cell types is distinct under phase-contrast optics. The level of filipin fluorescence, indicating membrane cholesterol content, was 2.3-fold higher in astrocytes compared to neurons (Fig. 1A; $n = 156$ astrocytes and $n = 135$ neurons; $P < 0.001$). To establish protocols to manipulate membrane cholesterol levels in neurons and astrocytes, we used 24-h pretreatment of hippocampal co-cultures with 0.5 mM mevastatin, a competitive inhibitor of HMG-CoA reductase, the rate-limiting enzyme of cholesterol biosynthesis (Fig. 1B), 1 mM methyl-β-cyclodextrin (mβCD), a cyclic oligosaccharide that forms a complex with cholesterol because it has a central cavity that 'fits' cholesterol in plasma membranes (Fig. 1B) and incubation of the cells with 0.5 mM cholesterol or 0.5 mM water-soluble cholesterol balanced with mβCD for cholesterol–mβCD complexes to increase the cholesterol content of cell membranes. Mevastatin significantly reduced the level of cholesterol (measured with

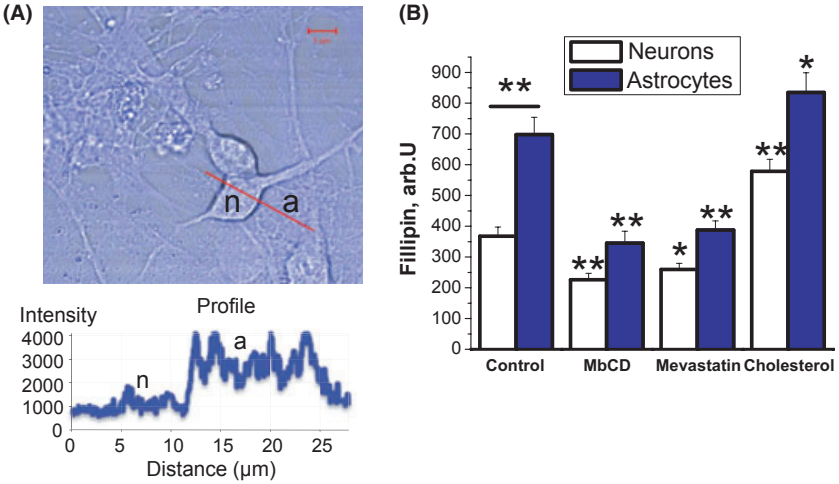

Fig. 1 Membrane cholesterol content differs between neurons and astrocytes in hippocampal co-cultures and can be modulated. The level of cholesterol in membranes of neurons and astrocytes was measured using fluorescence of filipin. (A) Merged transmitted image of neurons and astrocytes and filipin fluorescence (blue). Profile of filipin fluorescence along the line indicated in the image demonstrates the lower level of cholesterol in the neuronal membrane (*n*) compared to an adjacent astrocyte (a). (B) The level of cholesterol in hippocampal neurons and astrocytes in untreated cultures and incubated for 24 h with 0.5 mM cholesterol, 1 mM mβCD or mevastatin was measured as a mean filipin intensity projection from the z-stack. $^{**}P < 0.05$ and $^{***}P < 0.001$ vs. control. All data were expressed as mean ± SEM.

filipin fluorescence) in both neurons (to 72.9 ± 4.3% of control; $n = 57$; $P < 0.01$) and astrocytes (to 56.7 ± 3.7% of control astrocytes; $n = 82$; $P < 0.001$; Fig. 1B). Pretreatment of hippocampal co-cultures with mβCD also effectively decreased the concentration of cholesterol in the membranes of neurons (to 63.8 ± 5.1% of control neurons; $n = 49$; $P < 0.001$) and astrocytes (to 49.7 ± 3.1 of control; $n = 67$; $P < 0.001$; Fig. 1B). Both lipid- and water-soluble cholesterols significantly increased filipin fluorescence in both neurons and astrocytes. In neurons, the filipin fluorescence signal increased by 1.56-fold for lipid-soluble cholesterol ($n = 58$; $P < 0.05$; Fig. 1B) and by 1.44-fold for water-soluble cholesterol ($n = 37$; data not shown). The signal in astrocytes increased by 1.21-fold for the lipid-soluble cholesterol ($n = 89$; $P < 0.05$; Fig. 1B) and by 1.34-fold for the water-soluble cholesterol ($n = 56$; $P < 0.05$; data not shown).

Ca^{2+} fluctuations in response to βA require plasma membrane cholesterol

In agreement with our previous observation, exposure of primary hippocampal co-cultures with βA 1–42 (5 μM) or βA 25–35 (50 μM) induced $[Ca^{2+}]_c$ changes in astrocytes ($n = 55$) but not in neurons ($n = 37$; Fig. 2A). Decreasing membrane cholesterol by pretreatment of the cells with mβCD abolished the $[Ca^{2+}]_c$ signals in astrocytes in response to 50 μM βA 25–35 ($n = 58$; Fig. 2B) or 5 μM βA 1–42 ($n = 64$; data not shown) while no change in response was seen in adjacent neurons in the co-cultures. Filipin, which we used as a fluorescent probe to assess cholesterol levels, is a polyene macrolide antibiotic that binds to membrane sterols, such as cholesterol, and disrupts raft structure (Kojro *et al.*, 2001). Hence, this agent also can be used to deplete membrane cholesterol acutely. Application of low concentrations of filipin (0.5 μM) did not change $[Ca^{2+}]_c$ levels of neurons or astrocytes but blocked the effect of βA 1–42 and βA 25–35 on $[Ca^{2+}]_c$ of astrocytes ($n = 62$; Fig. 2C). It should be noted that at higher concentrations, filipin (5 μM) induced $[Ca^{2+}]_c$ signals in the majority of hippocampal neurons and astrocytes (Fig. 2D). Consecutive addition of filipin followed by 5 μM βA 1–42 induced a massive increase in $[Ca^{2+}]_c$ in both astrocytes and neurons that led to cell lysis (note the collapse of some calcium traces from single cells shown in Fig. 2D), presumably by causing a degree of membrane disruption, although the intracellular dye did not leak from the cells, and so this was not a true permeabilization ($n = 78$ astroctes, $n = 42$ neurons). Thus, a modest decrease in the level membrane cholesterol in astrocytes abolished βA-induced $[Ca^{2+}]_c$ signals. To investigate whether an

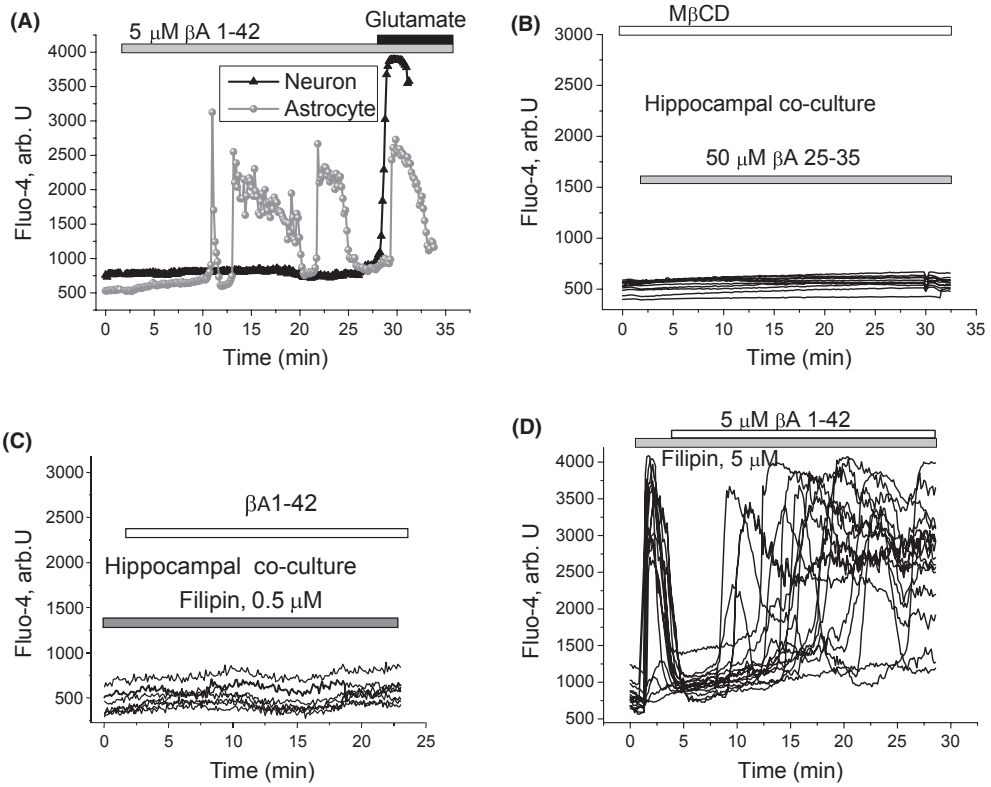

Fig. 2 Decreased membrane cholesterol protects hippocampal co-cultures against βA-induced calcium signals. (A) βA 1–42 (5 μM) induces calcium signal in astrocytes but not in neurons from primary hippocampal co-culture. Neuronal identity was confirmed by the cellular response to glutamate (50 μM) applied at the end of experiment. Decrease in the level of membranal cholesterol with 24-h pre-incubation of cells with 1 mM mβCD (B) or by binding of cholesterol with 0.5 μM filipin (C) protected astrocytes against βA-induced calcium signals. (D) a high concentration of filipin (5 μM) stimulates $[Ca^{2+}]_c$ in neurons and astrocytes and makes these cells more sensitive to the effect of βA on $[Ca^{2+}]_c$.

increased membrane cholesterol concentration can modify the $[Ca^{2+}]_c$ responses to βA in neurons and astrocytes, we preloaded hippocampal co-cultures with cholesterol, increasing membrane cholesterol as confirmed by an increase in the intensity of filipin fluorescence in both astrocytes and neurons (Fig. 1B).

Even short incubation (1 h) of the cells with 0.5 mM lipid-soluble cholesterol significantly increased the level of membrane cholesterol (1.7-fold for neurons; $n = 24$; $P < 0.001$; 1.45-fold for astrocytes; $n = 34$; $P < 0.05$; data not shown). Increasing membrane cholesterol content in hippocampal neurons using either lipid-soluble or water-soluble cholesterol (1 h pre-incubation, 0.5 mM) significantly increased the probability of that βA would initiate $[Ca^{2+}]_c$ signals in these cells. Thus, 5 μM βA 1–42 initiated calcium signals in 77 neurons of 81 tested (Fig. 3A) and 50 μM βA 25–35 in 40/42 neurons (Fig. 3B), while in control neurons, both short- and full-length peptide failed to induce any detectable calcium signal in all of 37 neurons tested (βA 1–42; $n = 42$ for βA 25–35 (Fig. 2A). Thus, it is clear that the level of membrane cholesterol plays a key role in determining the $[Ca^{2+}]_c$ responses of neurons and astrocytes.

Modification of cholesterol concentration could change the activity of extant ion channels, or it might influence the incorporation of βA into biological membranes as a pore-forming peptide. To determine whether cholesterol effects incorporation of βA into membranes, we used artificial membranes in which we varied the cholesterol content.

βA 1–42 and βA 25–35 increase calcium permeability in unilamellar vesicles

To investigate the ability of βA to incorporate into membranes and form Ca^{2+} permeant channels, a large unilamellar liposomes formed from lipids with or without cholesterol loaded with 10 mM $CaCl_2$ were used. Increased permeability of membranes for Ca^{2+} was registered as the release of calcium into the buffer, detected by the fluorescence of fura-2 included in the buffer.

Addition of the full peptide βA 1–42 (10 μM) or the fragment βA 25–35 (10 μM) induced a significant increase in the fura-2 ratio (Fig. 4A,B), indicating calcium efflux from the liposomes. Incorporation of βA 1–42 and βA 25–35 into membranes was dependent on the presence of cholesterol in the membrane of the liposomes. Thus, the permeability coefficient for cholesterol containing liposomes in response to βA 1–42 was 2-fold higher compared to liposomes formed with cholesterol-free membranes ($n = 3$; $P < 0.05$; Fig. 4A). The amplitude of βA 25–35–stimulated calcium release from cholesterol containing

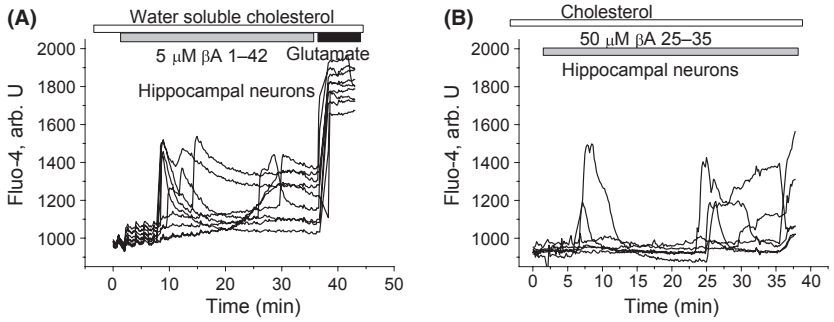

Fig. 3 Increased membranal cholesterol in hippocampal neurons supports βA-induced calcium signals. Increased concentration of cholesterol in the membranes of hippocampal neurons by pre-incubation of the cells with water-soluble 0.5 mM cholesterol (water-soluble cyclodextrin complexes, (A) or with lipid-soluble cholesterol (0.5 mM, B) made the cells more vulnerable to βA-induced calcium signals. To confirm the neuronal identity, 50 μM glutamate was added at the end of each experiment.

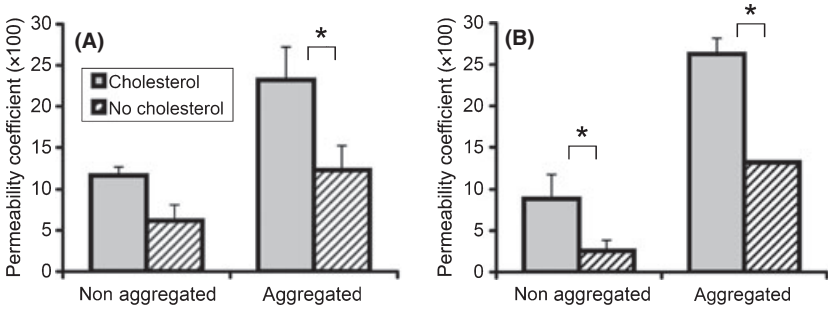

Fig. 4 βA-induced calcium permeability of liposomes is dependent on cholesterol. Calcium permeability coefficients were registered as amplitude of release of calcium from liposomes (F340/F380 ratio) in response to βA and calculated as described in the Methods section. Large unilamellar vesicles were prepared from PC/Chol/PE/PS/SM, 55:25:10:5:5, (Mol/Mol) or PC/PE/PS/SM, 80:10:5:5, (Mol/Mol). Panel A represents data for 10 μM βA 1–42; Panel B for 10 μM βA 25–35. The error bars are expressed as means ± SD.

liposomes was 2.1-fold higher compared to liposomes without cholesterol (n = 4; Fig. 4B).

The ability of βA to incorporate into the membrane and to form channels is dependent on the aggregation of the peptide (Hirakura *et al.*, 2000; Demuro *et al.*, 2005). We therefore used aggregated and nonaggregated βA peptides as a positive control in our experiments (Fig. 4A,B). Note the significant difference in permeability of liposomal membranes between nonaggregated and aggregated peptides. These results confirm affinity of this method for comparative analysis of βA-induced membrane permeability.

βA-induced channel formation in artificial lipid bilayers is cholesterol dependent

We also tested whether the presence of cholesterol influences the channel-forming properties of βA peptide. The presence of βA peptides in the recording solution induced the appearance of channel activity in artificial lipid bilayers, which was not observed when membranes were formed in the absence of the peptide. Channel activity was observed either in the presence or in the absence of cholesterol, i.e. when bilayers were formed with POPE lipids or with a mix of POPE and cholesterol (10:1 w/w). In both cases, complicated channel behaviour was observed with multiple conductance levels and transition steps. Similar channel activity was observed when both full-length βA 1–42 (5 μM) and the short peptide βA 25–35 (50 μM) were used. Figure 5A shows typical single-channel recording obtained in the presence of βA 25–35 on the membranes with cholesterol. In some experiments, integral conductances presumably caused by several consecutive channel incorporations were detected (Fig. 5B). Observed channel activity did not demonstrate any obvious voltage dependence (Fig. 5C). To compare channel activity between control and cholesterol-containing bilayers, we analysed the maximal membrane conductances observed when bilayers were formed either in the presence or in the absence of cholesterol in solutions containing 50 μM of βA 25–35. In the absence of cholesterol, channel activity was observed in 48% of experiments (21 of 44). In the presence of cholesterol, channel detection frequency increased to 91% of experiments (39 of 43 experiments). The average conductance of the bilayers, which is directly proportional to the amount of channels formed in the presence of βA, was also significantly higher in membranes containing cholesterol at 1.9 ± 0.3 nS, n = 43 compared to 0.6 ± 0.1 nS, n = 44 in control (POPE only membrane). Figure 5D illustrates the distribution of membrane conductance in the two groups of experiments (with and without cholesterol) – note the significant increase in membrane conductance in the presence of cholesterol. Overall, we conclude that cholesterol significantly facilitates the channel-forming activity of βA peptide in lipid membranes.

Cell death in response to βA is increased by high membrane cholesterol

The effect of altering plasma membrane cholesterol on cell viability after incubation with βA 1–42 was investigated in co-cultures of hippocampal neurons and astrocytes. Exposure of mixed hippocampal culture to 5 μM βA 1–42 (24 h) caused death of 51.9 ± 4.9% of neurons and 33.8 ± 3.1% of astrocytes (n = 5 experiments; Fig. 6A). Elevating cholesterol levels in the plasma membrane by incubation with added cholesterol significantly increased cell death to 72.7 ± 6.8% for neurons and to 48.9 ± 4.7% for astrocytes (P < 0.001; n = 3 experiments),

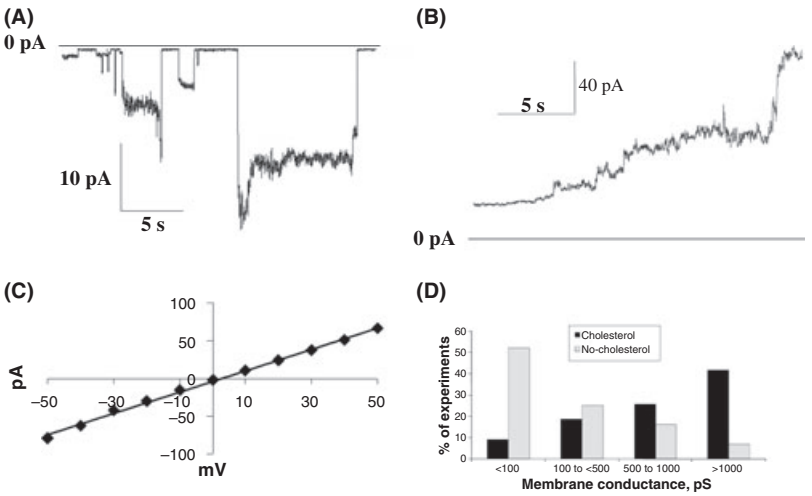

Fig. 5 βA channel activity in artificial lipid bilayers. Representative channel activity recorded from cholesterol-containing lipid bilayer membrane in the presence of A-beta peptide. Lipid bilayers were formed in recording solution containing 150 mM KCl, 5 mM $MgCl_2$ and 5 mM Tris–HEPES pH = 7.4 in the presence of 5 micro-βA 25–35 peptide. (A) Representative single-channel activity recorded at –50 mV showing characteristic transitions from fully closed state to various sub-conductance levels. (B) Integral conductance induced by incorporation of multiple channels. (C) Current–voltage relationship of the maximal conductance state of the channel. (D) Distribution of the detection frequencies of maximal conductance values observed in separate experiments, based on the analysis of 39 recordings in the presence and 21 recordings in the absence of cholesterol.

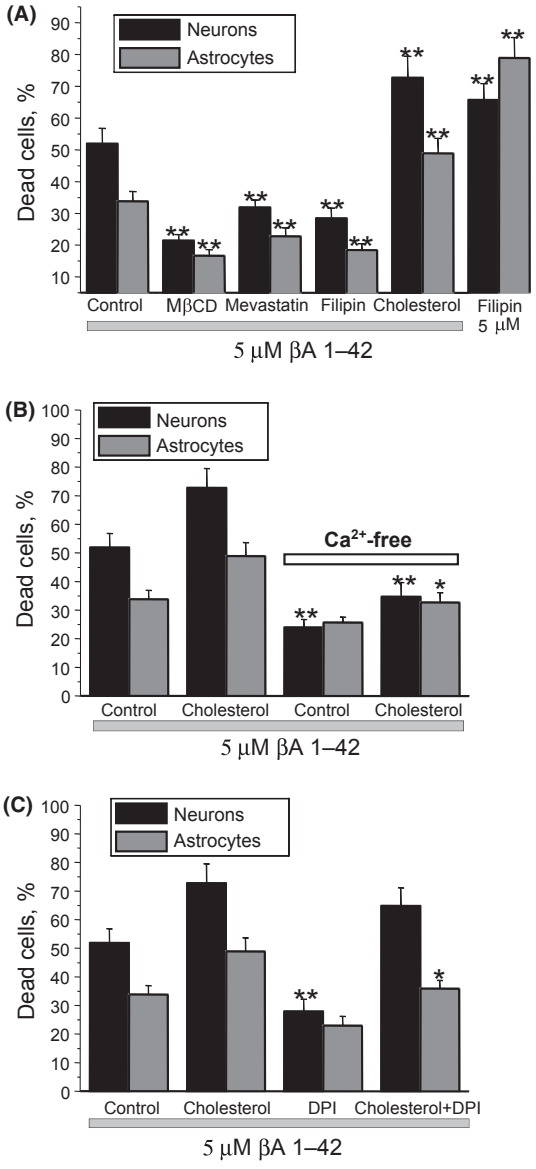

Fig. 6 βA-caused, Ca^{2+}-induced cell death is dependent on the level of cholesterol in the membrane of neurons and astrocytes. Effect of βA on viability of neurons and astrocytes. (A) PI fluorescence was used to detect dead cells 24 h after addition of βA 1–42 (5 μM) to the cell cultures pretreated with 0.5 mM cholesterol (n = 3 experiments), 1 mM mβCD (n = 4), mevastatin (n = 4) or filipin (0.5 μM, n = 5). Dead cells were counted with respect to the total number of cells present, identified by staining nuclei with Hoechst 33342. βA caused a dramatic increase in cell death in neurons (P < 0.001) and astrocytes (P < 0.001) in hippocampal co-cultures that was decreased by depletion of membrane cholesterol and increased by supplementing membrane cholesterol. Higher concentrations of filipin (>5 μM) significantly (n = 3 experiment; P < 0.001) increased the numbers of dead cells in co-cultured neurons and astrocytes even without βA treatment. (B) Treatment of cells in a Ca^{2+}-free medium significantly protected neurons and astrocytes from the toxicity of βA 1–42 (5 μM). (C) Pretreatment (20 min and during the experiment) of co-cultured hippocampal neurons and astrocytes with the NADPH oxidase inhibitor 0.5 μM DPI protected native neurons from βA-induced cell death, but failed to protect neurons with increased membrane cholesterol. **P < 0.05 and ***P < 0.001 vs. βA-treated control or untreated control for 5 μM filipin. All data were expressed as mean ± SEM.

indicating that higher cholesterol levels increase the vulnerability of these cells to the toxic effects of βA 1–42.

Similarly, decreasing plasma cholesterol was protective against βA 1–42 toxicity. Pre-incubation of the cells with either mβCD, 0.5 μM filipin or mevastatin all greatly and significantly reduced Aβ-induced toxicity (Fig. 6A). Thus, MβCD decreased cell death in both cell types by ~2-fold (n = 4; P < 0.001). Filipin reduced the neuronal death to 28.4 ± 3.3% (compared to 51.9 ± 4.9%; n = 5; P < 0.001), while mevastatin reduced neuronal death to 31.8 ± 2.4% (n = 4; P < 0.001). It should be noted that high concentrations of filipin (5 μM) that increased the calcium signals (Fig. 2D) significantly increased the number of dead neurons (to 65.7 ± 5.1% from a basal level of 11.7 ± 0.9% in the untreated controls, n = 3 experiments; P < 0.001; Fig. 6A) and astrocytes (to 78.9 ± 6.4% compared to a control of 12.9 ± 1.1%; n = 3; P < 0.001; Fig. 6A).

In agreement with our previous publication (Abramov *et al.*, 2003), removal of Ca^{2+} from the medium significantly (P < 0.001) protected the hippocampal neurons (cell death fell from 51.9 ± 4.9% to 23.9 ± 2.8, n = 3 experiments; Fig. 6B) and, to a lesser degree, the astrocytes in co-culture (from 33.8 ± 3.1% to 25.7 ± 1.9%, n = 4 experiments; Fig. 6B). Importantly, the absence of Ca^{2+} in medium significantly protects cells with high cholesterol against toxicity of βA 1–42 (Fig. 6B). Thus, the number of dead cells in cholesterol-treated neurons was reduced from 72.7 ± 6.8% to 34.6 ± 5% (n = 4; P < 0.001; Fig. 6B), strongly suggesting a link between the βA-induced calcium signal in cholesterol-incubated neurons and subsequent cell death. The presence or absence of Ca^{2+} in the medium did not alter cell death in cells that were untreated.

Previously, we demonstrated that βA toxicity in neurons is induced by the calcium-dependent activation of the NADPH oxidase in astrocytes (Abramov *et al.*, 2004a; Abramov & Duchen, 2005). In the present series of experiments, we found that the NADPH oxidase inhibitor, DPI (0.5 μM; 20-min pre-incubation), significantly reduced βA-induced neuronal cell death from 51.9 ± 4.9% to just 27.9 ± 4.3 (n = 3; P < 0.001; Fig. 6C). However, in cholesterol-rich neurons, in which βA now induced a $[Ca^{2+}]_c$ signal, the protective effect of DPI was very much reduced (cell death was reduced from 72.7 ± 6.8% to 64.8 ± 6.3%, n = 4; Fig. 6C), suggesting that the direct elevation of neuronal $[Ca^{2+}]_c$ by βA in cells with a high membranal cholesterol may itself be sufficient to induce cell death and bypass the role of the astrocytic NADPH oxidase.

Discussion

We have found that the cholesterol content in the membrane of hippocampal neurons is lower compared to neighbouring astrocytes in the same co-culture. It is important to emphasize that the membrane cholesterol content is independent of cholesterol levels in the circulation, as the cholesterol in lipoprotein particles does not pass through the established blood–brain barrier in adults. Cholesterol in the brain is mainly synthesized by oligodendrocytes and astrocytes. Whereas oligodendrocytes produce

cholesterol required for myelination, astrocytes also produce cholesterol at 2–3 times greater amounts than that produced from neurons for ATP-binding cassette transporters (Bjorkhem & Meaney, 2004), and our new data suggest that this is reflected in substantial differences in the membrane cholesterol content between these cell types.

High membrane cholesterol content facilitates the formation of a βA–GM1 ganglioside complex that can act as a seed for consecutive binding of βA and aggregate formation in AD brains (Hayashi *et al.*, 2004). It can also serve as a basis for βA pore formation, as confirmed by our experiments. We found that lowering cholesterol levels in the membrane of astrocytes and neurons prevented βA-induced calcium signalling and dramatically protected cells from cell death, while elevation of cholesterol in the membrane of these cells supported calcium signalling in response to βA in both cell types. We obtained similar results using artificial membranes in both liposomes and black lipid membranes (BLM), supporting a direct link between the level of membrane cholesterol, the incorporation of βA into the membrane and its ability to form a calcium permeant pore. This βA pore formation in cholesterol-rich membranes induced a $[Ca^{2+}]_c$ signal that was sufficient to cause neuronal and astrocytic death and was prevented simply by preventing the $[Ca^{2+}]_c$ signal by the removal of extracellular Ca^{2+} (Fig. 6B). Importantly, increased membranal cholesterol in neurons facilitated the incorporation of βA into neuronal membranes and also increased Ca^{2+} induced cell death (much as described for astrocytes – see (Abramov *et al.*, 2007)). This was distinct from native neurons that were not exposed to cholesterol, in which calcium signals were absent (Fig. 6C; see also Abramov *et al.*, 2003, 2004a).

Digitonin and other saponins bind membranal cholesterol, and the complex cholesterol–digitonin forms a pore (Leung *et al.*, 1997). It is less likely that βA forms the same complexes with cholesterol because of the differences in chemical structures and molecular mass with digitonin, but same principle as in case of this saponins (binding to the cholesterol in membranes) may take a place in case of amyloid. We also can share the observation from our experience that digitonin permeabilizes astrocytes much faster and in lower concentration compared to neighbouring neurons.

It is possible that in our experiments with BLM and liposomes, the presence of cholesterol changes membrane properties in such a way that it facilitates βA binding to the membrane and/or formation of ion channels as suggested before by other groups (Micelli *et al.*, 2004). This is consistent with previous experiments, which suggest that cholesterol potentiates βA binding to lipid membranes. It should be noted, however, that some of the published data suggest that *increased* cholesterol inhibits channel formation (Lin & Kagan, 2002). Although our data obtained on artificial membranes are consistent with the facilitation of channel formation by cholesterol, it is also possible that in the cell models, cholesterol-induced activation occurs through yet unidentified mechanism that involves other membrane components.

Considering this, we propose that high concentrations of cholesterol change the membrane composition, supporting the incorporation of βA into the membrane where it forms a pore. Interestingly, more profound binding of cholesterol with high dose of filipin also supports βA pore formation, as observed by Arispe & Doh (2002).

As we demonstrated earlier (Abramov *et al.*, 2003, 2004b), βA does not induce calcium signals in neurons in ''healthy'' cultures or brain slices. Age-related increases in the cholesterol level of biological membranes (Wood *et al.*, 2009; Martin *et al.*, 2010) may increase the risk of incorporation of aggregated βA into neurons and induced neurodegeneration.

Experimental procedures

Peptides and treatments

βA 25–35, βA 1–42 and βA 35–25 (Bachem, St. Helens, UK) were dissolved at 1 mM in sterile HSBS (Invitrogen, Paisley, UK) and kept frozen until use. The peptides were added under the microscope, except for neurotoxicity measurements, where they were added 24 h before the experiment. βA 1–42 was used at concentration 5 μM, and βA 25–35 was used at concentrations of up to 50 μM to ensure that it was present in molar excess compared to inhibitors and so excludes any direct interaction.

Cell culture

Mixed cultures of hippocampal neurons and glial cells were prepared as described previously (Abramov *et al.*, 2003) with modifications, from Sprague-Dawley rat pups 2–4 days post-partum (UCL breeding colony). Hippocampi were removed into ice-cold Ca^{2+}-free HBSS (Invitrogen). The tissue was minced and trypsinized (0.1% for 15 min at 37°C), triturated and plated on poly-D-lysine-coated coverslips and cultured in Neurobasal medium (Invitrogen) supplemented with B-27 (Invitrogen) and 2 mM L-glutamine. Cultures were maintained at 37°C in a humidified atmosphere of 5% CO_2 and 95% air, fed twice a week and maintained for a minimum of 10 days before experimental use to ensure the expression of glutamate and other receptors. Neurons were easily distinguishable from glia: they appeared phase bright, had smooth rounded somata and distinct processes and lay just above the focal plane of the glial layer. Cells were used at 10–20 days *in vivo* (DIV) unless differently stated.

Microscopy

Confocal images were obtained using a Zeiss 510 CLSM and a 40× oil immersion objective. The 488-nm Argon laser line was used to excite fluo-4 fluorescence that was measured using a bandpass filter from 505 to 550 nm. Filipin fluorescence was excited at 351 and measured at 420–470 nm. Illumination intensity was kept to a minimum (at 0.1% of laser output) to avoid phototoxicity and the pinhole set to give an optical slice of ~2 μm.

$[Ca^{2+}]_c$ measurements

Cells were loaded for 30 min at room temperature with 5 μM fluo-4 AM (Molecular Probes, Eugene, OR, USA) and 0.005% Pluronic in a HEPES-buffered salt solution (HBSS) composed of (mM) 156 NaCl, 3 KCl, 2 $MgSO_4$, 1.25 KH_2PO_4, 2 $CaCl_2$, 10 glucose and 10 HEPES, pH 7.35. Data are presented normalized with respect to the first image of the sequence. All presented data were obtained from at least five coverslips and 2–3 different cell preparations.

Liposome preparations

Large unilamellar vesicles (LUV) composed of PC/Chol/PE/PS/SM, 55:25:10:5:5, (Mol/Mol) or PC/PE/PS/SM, 80:10:5:5, (Mol/Mol) were prepared using the thin-film hydration method. Briefly, appropriate amounts of lipid solutions in chloroform were placed in a round-bottom flask, and the thin lipidic film was formed by slow removal of the solvent under argon atmosphere. The remaining solvent traces were removed under vacuum using a rotary evaporator over a water bath at 37°C for 30 min. The resulting lipid film on the wall of the flask was hydrated with an appropriate volume of buffer containing 10 mM of $CaCl_2$ resulting in a final lipid concentration of 5 mg mL^{-1}. The mixture was vortexed for 5 min with glass beads and allowed to equilibrate for 30 min under argon atmosphere at 37°C (above the gel-liquid crystal transition temperature of the lipid mixture). Subsequently, the liposome suspension was forced to pass at least 15 times through a polycarbonate membrane of 400 nm porosity (Nuclepore, T-E), mounted in a mini-extruder (Avanti Polar Lipids, Alabaster, Alabama, USA) fitted with two 1000-μL Hamilton gastight syringes. Exposure to light was minimized throughout the liposome preparation process. For removing the excess of Ca^{2+}, the liposomal suspension was passed through column containing Sephadex G-25 (Sigma, Sigma-Aldrich, St. Louis, MO USA).

The size distribution (*z*-average mean) and polydispersion index of the liposomes were measured at room temperature using dynamic light scattering in a photon correlation spectrometer (Zetasizer Nano-S90, Malvern Instruments, Malvern UK). The refraction factor was assumed 1.336 while the detection angle was 90'' and the wavelength was 633 nm. The analysis method used was based on CONTIN algorithm.

Single-channel recordings

Bilayers were formed across an aperture of 100–200 μm diameter in the wall of a Teflon cup (Warner Instruments) by painting with POPE lipids (Avanti) diluted in decane to the concentration of 10 mg lipid mL^{-1} as described earlier (Pavlov *et al.*, 2005). In some experiments, POPE lipids were supplemented with cholesterol to the final ratio by weight 1:10 (cholesterol:POPE). βA 1–42 peptide was added directly to the recording solution to the final concentration of 5 μM. Recording solution contained 150 mM KCl, 5 mM MgCl2 and 5 mM Tris–HEPES. All solutions were adjusted to pH 7.4. Data were collected with Axopatch-1B amplifier, filtered at 100 Hz (−3 dB, low pass, 4-pole Bessel filter) and digitally recorded to PC, using pClamp 9.0 software (Axon Instruments, Union City, CA, USA). Most analysis was performed with the same software.

Calcium efflux measurements in liposomes (determination of calcium permeability)

Fura-2 fluorescence was measured on a Perkin Elmer LS 50B (Seer Greek, Buckinghamshire, UK) spectrofluorimeter. The excitation slit width was 2.5 nm; the emission wavelength was 510 nm with a slit width of 5 nm. Appropriated amount of concentrated Ca^{2+}-entrapped LUVs was added to the Fura-2 (2 μM) buffer to a final volume of 2000 μL at 37°C. The rate of calcium efflux was monitored by following the changes in the fluorescence ratio of Fura-2 at excitation wavelengths of 340 nm and 380 nm (F340/F380). The calcium permeability coefficient, *P*, can be calculated from the equation:

$$P = \frac{R_s - R_{min}}{R_{max} - R_{min}}$$

where *R* is F340/F380. R_{min} and R_{max} were obtained by adding excess EGTA and Ca^{2+} after treatment with 0.5% Triton X-100. R_s was obtained by adding of 10 μM of β-amyloid.

Toxicity experiments

For toxicity assays, we loaded cells simultaneously with 20 μM propidium iodide (PI), which is excluded from viable cells but exhibits a red fluorescence following a loss of membrane integrity, and 4.5 μM Hoechst 33342 (Molecular Probes), which gives a blue staining to chromatin to count the total number of cells. Using phase-contrast optics, a bright-field image allowed identification of neurons, which look quite different to the flatter glial component and also lie in a different focal plane, above the glial layer. A total number of 600–800 neurons or glial cells were counted in 20–25 fields of each coverslip. Each experiment was repeated five or more times using separate cultures.

Statistical analysis

Statistical analysis and exponential curve fitting were performed using Origin 8 (Microcal Software Inc., Northampton, MA, USA) software. Results are expressed as means ± standard error of the mean (SEM).

Acknowledgments

This work was supported by Clinical Research and Development Committee grant. We thank Dr. French (University of Calgary) for use of the bilayer set-up.

References

Abramov AY, Duchen MR (2005) The role of an astrocytic NADPH oxidase in the neurotoxicity of amyloid beta peptides. *Philos. Trans. R Soc. Lond. B Biol. Sci.* **360**, 2309–2314.

Abramov AY, Canevari L, Duchen MR (2003) Changes in intracellular calcium and glutathione in astrocytes as the primary mechanism of amyloid neurotoxicity. *J. Neurosci.* **23**, 5088–5095.

Abramov AY, Canevari L, Duchen MR (2004a) beta-amyloid peptides induce mitochondrial dysfunction and oxidative stress in astrocytes and death of neurons through activation of NADPH oxidase. *J. Neurosci.* **24**, 565–575.

Abramov AY, Canevari L, Duchen MR (2004b) Calcium signals induced by amyloid beta peptide and their consequences in neurons and astrocytes in culture. *Biochim. Biophys. Acta* **1742**, 81–87.

Abramov AY, Fraley C, Diao CT, Winkfein R, Colicos MA, Duchen MR, French RJ, Pavlov E (2007) Targeted polyphosphatase expression alters mitochondrial metabolism and inhibits calcium-dependent cell death. *Proc. Natl Acad. Sci. USA* **104**, 18091–18096.

Arispe NELS, Doh MICH (2002) Plasma membrane cholesterol controls the cytotoxicity of Alzheimer's disease A{beta}P (1-40) and (1-42) peptides. *FASEB J.* **16**, 1526–1536.

Arispe N, Pollard HB, Rojas E (1993) Giant multilevel cation channels formed by Alzheimer disease amyloid beta-protein [A beta P-(1-40)] in bilayer membranes. *Proc. Natl Acad. Sci. USA* **90**, 10573–10577.

Bignall J (1993) APOE gene dose in Alzheimer's disease. *Lancet* **342**, 426.

Bjorkhem I, Meaney S (2004) Brain cholesterol: long secret life behind a barrier. *Arterioscler. Thromb. Vasc. Biol.* **24**, 806–815.

Citron M (2004) Strategies for disease modification in Alzheimer's disease. *Nat. Rev. Neurosci.* **5**, 677–685.

Demuro A, Mina E, Kayed R, Milton SC, Parker I, Glabe CG (2005) Calcium dysregulation and membrane disruption as a ubiquitous neurotoxic mechanism of soluble amyloid oligomers. *J. Biol. Chem.* **280**, 17294–17300.

Drabikowski W, Lagwinska E, Sarzala MG (1973) Filipin as a fluorescent probe for the location of cholesterol in the membranes of fragmented sarcoplasmic reticulum. *Biochim. Biophys. Acta* **291**, 61–70.

Dringen R, Hirrlinger J (2005) Glutathione pathways in the brain. *Biol. Chem.* **384**, 505–516.

Haass C, Selkoe DJ (2007) Soluble protein oligomers in neurodegeneration: lessons from the Alzheimer's amyloid [beta]-peptide. *Nat. Rev. Mol. Cell Biol.* **8**, 101–112.

Hardy J, Selkoe DJ (2002) The amyloid hypothesis of Alzheimer's disease: progress and problems on the road to therapeutics. *Science* **297**, 353–356.

Hayashi H, Kimura N, Yamaguchi H, Hasegawa K, Yokoseki T, Shibata M, Yamamoto N, Michikawa M, Yoshikawa Y, Terao K, Matsuzaki K, Lemere CA, Selkoe DJ, Naiki H, Yanagisawa K (2004) A seed for Alzheimer amyloid in the brain. *J. Neurosci.* **24**, 4894–4902.

Hirakura Y, Yiu WW, Yamamoto A, Kagan BL (2000) Amyloid peptide channels: blockade by zinc and inhibition by Congo red (amyloid channel block). *Amyloid* **7**, 194–199.

Kagan BL, Azimov R, Azimova R (2004) Amyloid peptide channels. *J. Membr. Biol.* **202**, 1–10.

Kawahara M, Kuroda Y, Arispe N, Rojas E (2000) Alzheimer's +/−amyloid, human islet amylin, and prion protein fragment evoke intracellular free calcium elevations by a common mechanism in a hypothalamic GnRH neuronal cell line. *J. Biol. Chem.* **275**, 14077–14083.

Kojro E, Gimpl G, Lammich S, M+Ñrz W, Fahrenholz F (2001) Low cholesterol stimulates the nonamyloidogenic pathway by its effect on the +/−secretase ADAM 10. *Proc. Natl Acad. Sci. USA* **98**, 5815–5820.

Leung YM, Ou YJ, Kwan CY, Loh TT (1997) Specific interaction between tetrandrine and Quillaja saponins in promoting permeabilization of plasma membrane in human leukemic HL-60 cells. *Biochim. Biophys. Acta* **1325**, 318–328.

Lin McA, Kagan BL (2002) Electrophysiologic properties of channels induced by A[beta]25-35 in planar lipid bilayers. *Peptides* **23**, 1215–1228.

Martin M, Dotti CG, Ledesma MD (2010) Brain cholesterol in normal and pathological aging. *Biochim. Biophys. Acta* **1801**, 934–944.

Masters CL, Simms G, Weinman NA, Multhaup G, Mcdonald BL, Beyreuther K (1985) Amyloid plaque core protein in Alzheimer disease and Down syndrome. *Proc. Natl Acad. Sci. USA* **82**, 4245–4249.

Micelli S, Meleleo D, Picciarelli V, Gallucci E (2004) Effect of sterols on [beta]-amyloid peptide (a[beta]p 1-40) channel formation and their properties in planar lipid membranes. *Biophys. J.* **86**, 2231–2237.

Norman AW, Demel RA, De Kruyff B, Van Deenen LLM (1972) Studies on the biological properties of polyene antibiotics: evidence for the direct interaction of filipin with cholesterol. *J. Biol. Chem.* **247**, 1918–1929.

Pavlov E, Zakharian E, Bladen C, Diao CT, Grimbly C, Reusch RN, French RJ (2005) A large, voltage-dependent channel, isolated from mitochondria by water-free chloroform extraction. *Biophys. J.* **88**, 2614–2625.

Wood WG, Schroeder F, Igbavboa U, Avdulov NA, Chochina SV (2009) Brain membrane cholesterol domains, aging and amyloid beta-peptides. *Neurobiol. Aging* **23**, 685–694.